A pH-correctable, DNA-based fluorescent reporter for organellar Calcium

Nagarjun Narayanaswamy[#1,2], Kasturi Chakraborty[#1,2*], Anand Saminathan[1,2], Elizabeth Zeichner[1], KaHo Leung[1,2], John Devany[3], Yamuna Krishnan[1,2*]

[1]Department of Chemistry, The University of Chicago, Chicago, Illinois 60637, USA.
[2]Grossman Institute of Neuroscience, Quantitative Biology and Human Behavior, The University of Chicago, Chicago, Illinois 60637, USA.
[3]Department of Physics, The University of Chicago, IL, 60637, USA

[#]These authors contributed equally to this work.

**Corresponding authors. Email:yamuna@uchicago.edu; kasturi@uchicago.edu*

Table S1. Sequences used to form *CalipHluor*, *CalipHluor*$_{Ly}$ and *CalipHluor*^{mLy}. D1 and D2 were used to form *CalipHluor*$_{Ly}$; OG-D1 and D2 were used to form *CalipHluor*^{mLy}. Bromo cytosines in D1 are underlined and highlighted in red. O1-A488, O2-A647 and O3 strands were used to form *CalipHluor*. Complimentary sequences are highlighted in matching colors.

Strand	Sequence information
D1	5'-Alexa 488-CC<u>C</u> CTA AC<u>C</u> CCT AAC C<u>C</u>C TAA C<u>C</u>C CAT ATA TAT CCT AGA ACG ACA GAC AAA CAG TGA GTC-3'
D2	5'-DBCO-GAC TCA CTG TTT GTC TGT CGT TCT AGG ATA /iAlexa 647N/AT ATT TTG TTA TGT GTT ATG TGT TAT-3'
O1-A488	5'-Alexa-488-CCCCAACCCCAATACATTTTACGCCTGGTGCC-3'
O2-A647	5'-CCGACCGCAGGATCCTATAAAACCCCAACCCC-Alexa 647-3'
O3-DBCO	5'-TTA TAG GAT CCT GCG GTC GG/iDBCON/ GGC ACC AGG CGT AAA ATG TA-3'
OG-D1	5'-Oregon Green-AT AAC ACA TAA CAC ATA ACA AAA TAT ATA TCC TAG AAC GAC AGA CAA ACA GTG AGT C-3'

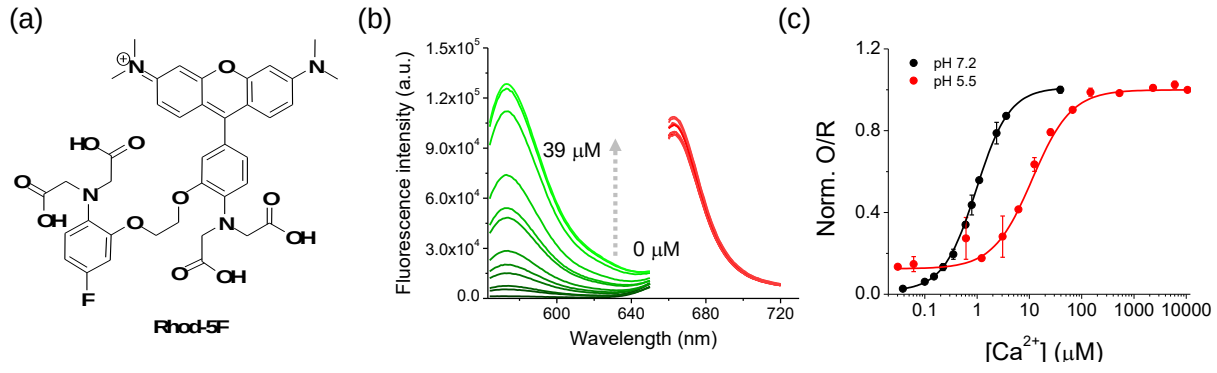

Figure S1. (a) Chemical structure of Rhod-5F. (b) Fluorescence emission spectra of Rhod-5F(green) and Alexa 647 (red) with increasing [Ca^{2+}] upon exciting Rhod-5F and Alexa647 at 560 nm and 650 nm respectively. (c) Normalized O/R ratio of Rhod-5F/Alexa 647 with increasing [Ca^{2+}] at pH 7.2 and 5.5. Error bar represents mean ± S.E.M of three independent experiments.

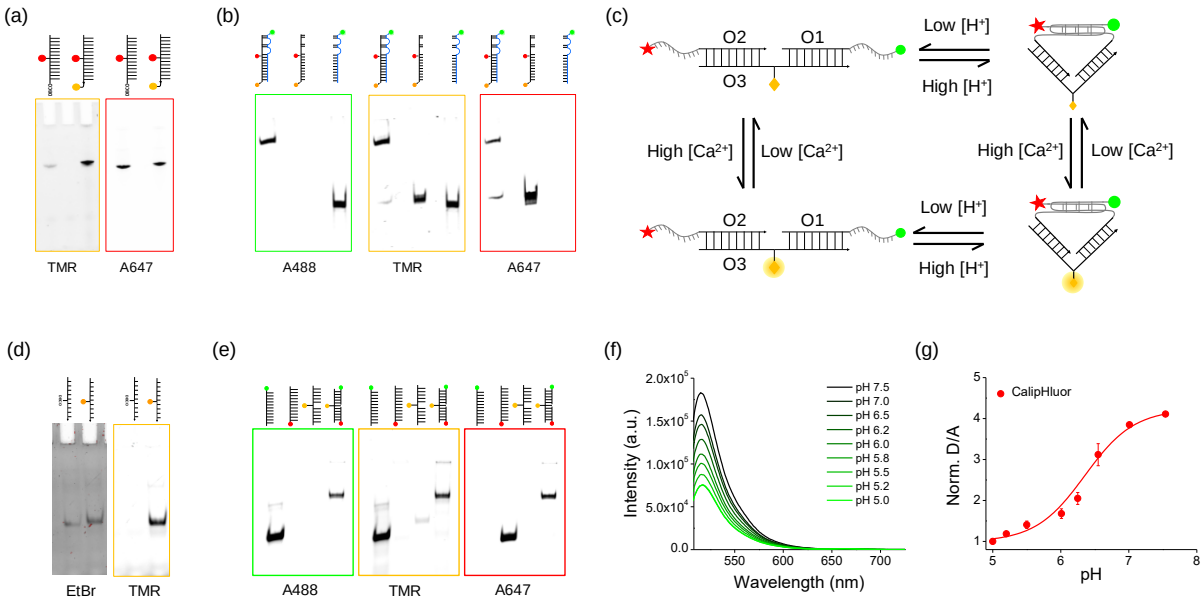

Figure S2. Characterization of *CalipHluor*$_{Ly}$ and *CalipHluor*. (a) Gel showing the conjugation of Rhod-5F to D2-DBCO strand. Gels were visualized in EtBr and TMR channels. (b) Native PAGE showing formation of *CalipHluor*$_{Ly}$. Gels were visualized in Alexa 488, TMR and Alexa 647 channels. (c) Schematic of working principle of *CalipHluor*. A pH-induced FRET changes between Alexa488 (donor, green sphere) and Alexa647 (acceptor, red star) is used to report pH ratiometrically. A Ca^{2+} sensitive fluorophore (Rhod-5F, yellow diamond) and Alexa647 report Ca^{2+} (at a given pH) ratiometrically by direct excitation of each dye. (d) Gel showing the conjugation of Rhod-5F to O3-DBCO strand. Gels were visualized in EtBr and TMR channels. (e) Native PAGE showing formation of *CalipHluor*. Gels were visualized in Alexa 488, TMR and Alexa 647 channels. (f) Emission spectra of *CalipHluor* at pH values ranging from 7.5 to 5.0 upon excitation at 488 nm. (g) Normalized ratio of fluorescence intensity of donor to that of acceptor (D/A) of *CalipHluor* as a function of pH. (D λ_{ex} = 495 nm, λ_{em} = 520 nm; A λ_{ex} = 495 nm, λ_{em} = 665 nm)**.** Gels were performed twice independently. Error bar represents mean $\pm$ S.E.M of three independent experiments.

The formation of *CalipHluor*$_{Ly}$ and *CalipHluor* were validated by electrophoretic mobility assay, using Native and Denaturing polyacrylamide gel electrophoresis (PAGE). Copper free click reaction of Rhod-5F-N_3 to DBCO labeled strand (D2 strand for *CalipHluor*$_{Ly}$ and O3-DBCO strand for *CalipHluor*) was validated by 15% denaturing PAGE run in 1X TBE, at 120 V for 3h. The

slower mobility of Rhod-5F conjugated strand, due to addition of 1 KDa (Rhod-5F) to 10 KDa (DBCO-strand). Rhod-5F conjugation was further confirmed by recording the gel in TMR channel, where the lower mobility band shows strong fluorescence. Rhod-5F labeled strand was purified and hybridized with normalizing and pH sensing module as described in methods section. 12% Native PAGE was run to characterize the formation of complete sensor. 12% Acrylamide: Bisacrylamide resolves duplex DNA from ssDNA. Slower mobility of *CalipHluor*$_{Ly}$ and *CalipHluor* owing to higher molecular weight validates the formation, at very high yield (> 99%). This further confirmed with slower mobility band, shows fluorescence at Alexa 488, TMR (Rhod-5F) and Alexa647 channel.

Table S2: Amount of free [Ca^{2+}] in clamping buffer at pH 5.5 was calculated using Maxchelator software.

Added calcium (μM)	Amount calcium added (μL)	Concentration of calcium added	Free [Ca^{2+}] (μM) in 50 μL
0	0	0	0
1	1	50 μM	3.89 E-2
2	2	50 μM	7.80 E-2
10	1	0.5 mM	3.89 E-1
20	2	0.5 mM	7.80 E-1
50	1	2.5 mM	1.9
100	2	2.5 mM	3.9
200	1	10 mM	7.9
500	1	25 mM	20.4
1E3	1	50 mM	43.1
2E3	2	50 mM	96.3
5E3	1	250 mM	360.3
10E3	2	250 mM	1.86 E3
20E3	2	500 mM	10.4 E03

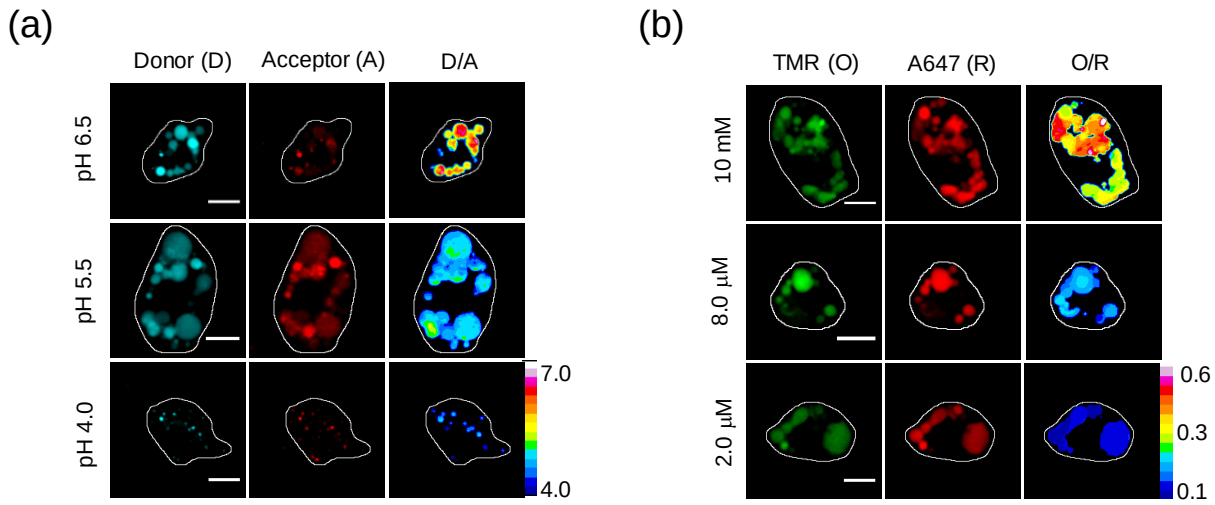

Figure S3. *In vivo* performance of *CalipHluor*$_{Ly}$. Representative pseudo color images of coelomocytes labeled with *CalipHluor*$_{Ly}$ and clamped at the indicated (a) pH and (b) free [Ca^{2+}] at pH 5.5. Scale bar 5 µm. Experiments were repeated thrice independently with similar results.

We performed *in vivo* calibration of *CalipHluor*$_{Ly}$ in lysosomes of coelomocytes and compare the performance w.r.t. *in vitro* calibration profiles. Lysosomes of coelomocytes were labeled with *CalipHluor*$_{Ly}$ as described in methods. Labelled lysosomes were clamped to equilibrate the lumenal ions with extracellular ions. This was achieved by using cocktail of specific ionophores that neutralizes the ionic gradient across the membrane and transport ion of choice. Nigericin and monensin ionophores were used to clamp pH, whereas ionomycin was used to clamp [Ca^{2+}] at lysosomes. Cocktail of these ionophores allow us to control the pH and Ca^{2+} levels in lysosomes and thus provides an accurate method to calibrate probes *in vivo*. Fluorescent images acquired in Donor, FRET channel and Rhod-5F, Alexa647 channel allow us to calibrate the intensity ratios for pH and [Ca^{2+}] respectively (Fig S3).

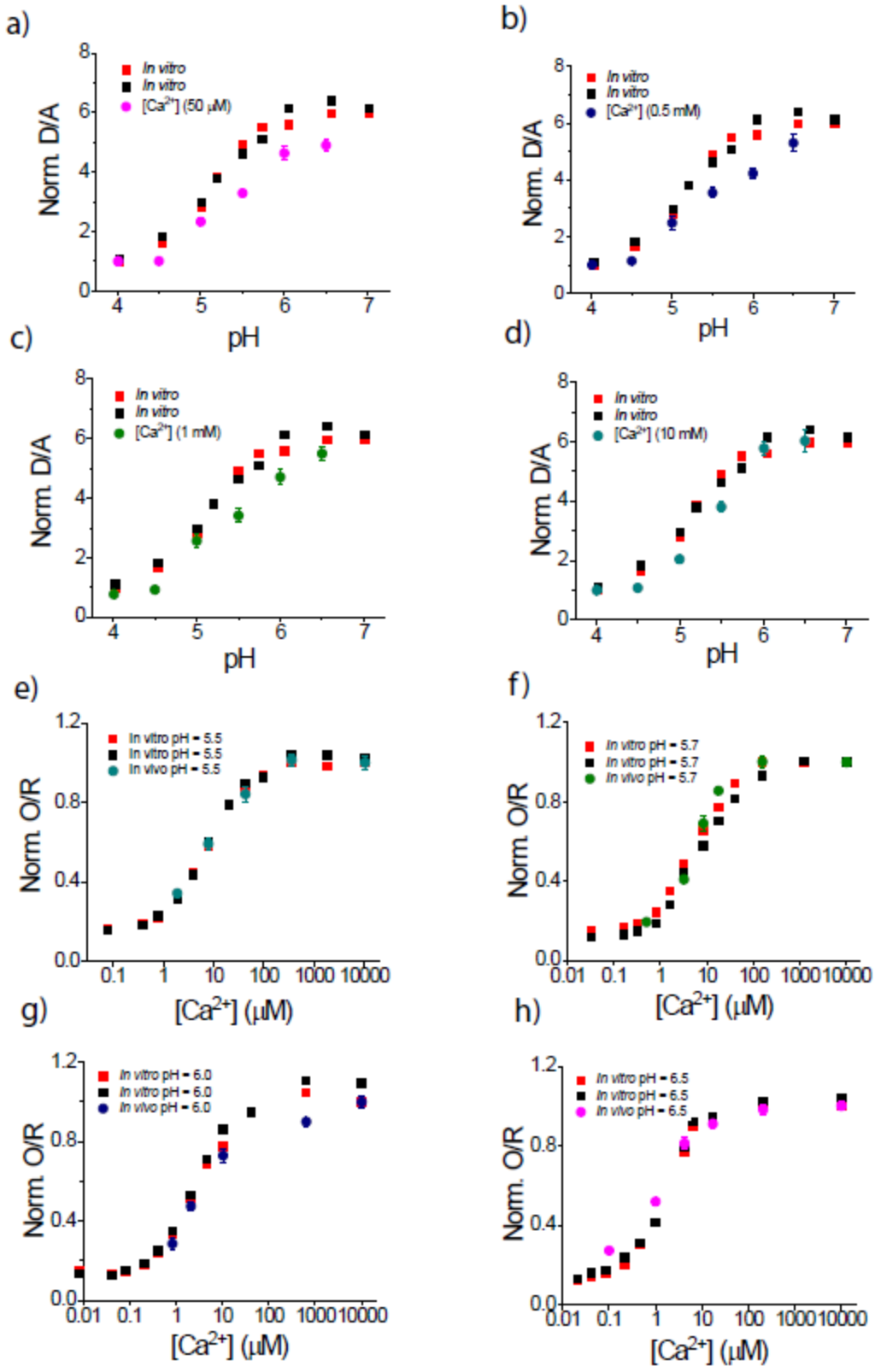
a)
Norm. D/A
pH
In vitro
In vitro
[Ca2+] (50 μM)
b)
Norm. D/A
pH
In vitro
In vitro
[Ca2+] (0.5 mM)
c)
Norm. D/A
pH
In vitro
In vitro
[Ca2+] (1 mM)
d)
Norm. D/A
pH
In vitro
In vitro
[Ca2+] (10 mM)
e)
Norm. O/R
[Ca2+] (μM)
In vitro pH = 5.5
In vitro pH = 5.5
In vivo pH = 5.5
f)
Norm. O/R
[Ca2+] (μM)
In vitro pH = 5.7
In vitro pH = 5.7
In vivo pH = 5.7
g)
Norm. O/R
[Ca2+] (μM)
In vitro pH = 6.0
In vitro pH = 6.0
In vivo pH = 6.0
h)
Norm. O/R
[Ca2+] (μM)
In vitro pH = 6.5
In vitro pH = 6.5
In vivo pH = 6.5

Figure S4. Comparison of *in vitro and in vivo* pH and Ca^{2+} calibration profile of *CalipHluor*$_{Ly}$. (a-d) D/A ratios of *CalipHluor*$_{Ly}$ as a function of pH clamped at different amounts of added [Ca^{2+}]. (e-h) Normalized O/R ratios of *CalipHluor*$_{Ly}$ as a function of free [Ca^{2+}] clamped at different pH points. For *in vivo* n=10 worms; 15 cells and 50 endosomes were considered; *in vitro* n=2. Error bar represents mean $\pm$ S.E.M.

The calibrated D/A and O/R ratios were calculated by measuring the intensity values at single lysosome resolution in all four channels, as described in methods. Plotting D/A against pH values, at different Ca^{2+} concentration shows the insensitivity of pH sensing module towards Ca^{2+} levels. Figure S4 (a-d) shows the comparison of D/A vs pH plots at different Ca^{2+} levels between *in vitro* and *in vivo*. Non-significant change in fold change and $pH_{1/2}$, shows the robustness of the sensor performance in biological systems.

In vivo Ca^{2+} clamping of coelomocytes was performed in Ca^{2+} clamping buffer [HEPES (10 mM), MES (10 mM), sodium acetate (10 mM), EGTA (10 mM), KCl (140 mM), NaCl (5 mM) and $MgCl_2$ (1 mM)] by varying amount of free [Ca^{2+}] from 1 μM to 10 mM and adjusting pH (5.5-6.5) in presence of nigericin (50 μM), monensin (50 μM) and ionomycin (20 μM). Because of difficulty clamping coelomocytes below 1 μM of free [Ca^{2+}], clamping points <1 μM were extrapolated from the *in vivo* calibration to get the K_d of *CalipHluor*$_{Ly}$ at pH 6.5 and 5.7. As shown in Figure S4 (e-h), *in vivo* [Ca^{2+}] calibration profiles of *CalipHluor*$_{Ly}$ correspond well with *in vitro* calibration profiles from pH 5.5 to 6.5 and from 1 μM to 10 mM of free [Ca^{2+}]. Further, *in vivo* K_d values of *CalipHluor*$_{Ly}$ as function of pH were consistent with *in vitro* K_d values (Fig. 2j). These results confirm that pH and [Ca^{2+}] sensing properties of *CalipHluor*$_{Ly}$ were preserved in coelomocytes.

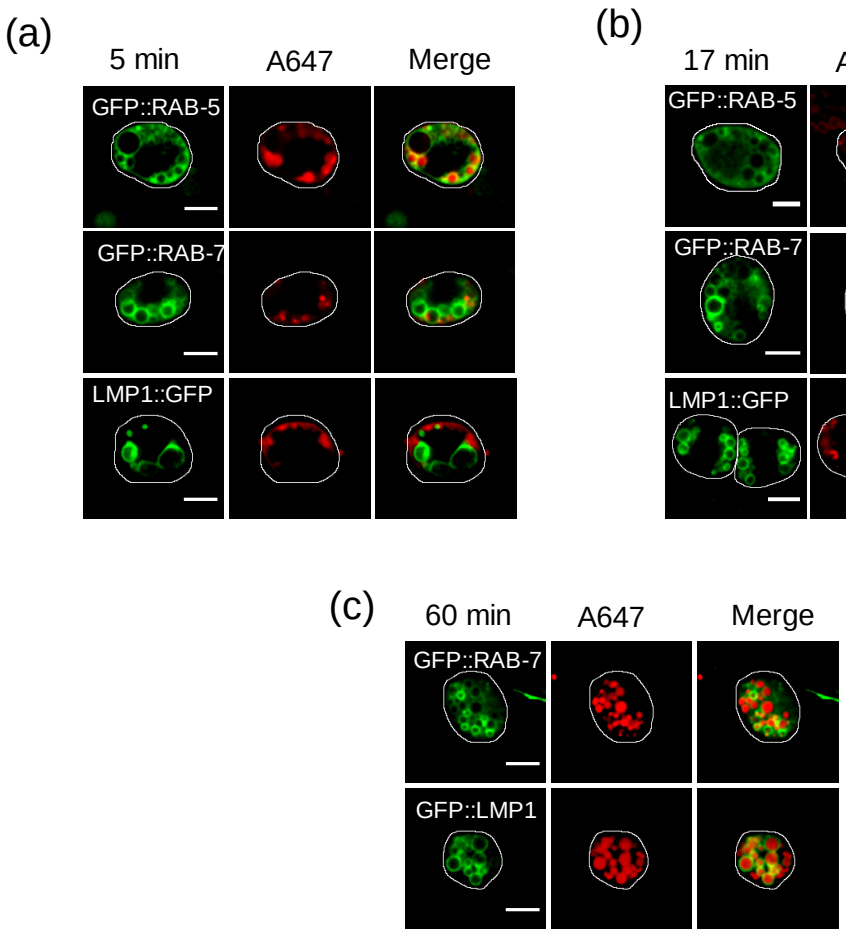

Figure S5. Endocytic trafficking of *CalipHluor*$_{A647}$ in coelomocytes. (a-c) Representative confocal images taken 5 min, 17 min, and 60 min following injection of *CalipHluor*$_{A647}$ in worms expressing GFP::RAB-5, GFP::RAB-7 and LMP-1::GFP. Scale bar 5 μm. Experiment was performed once in n=10 worms.

In receptor mediated endocytosis, endocytosed cargo traffics through the early endosomes (EE) and late endosomes (LE) to reach lysosomes (Ly) for degradation and recycling. To find out estimated time points of *CalipHluor*$_{A647}$ to reach EE, LE and Ly, time dependent colocalization experiments were performed in worms expressing GFP tagged endosomal markers GFP::RAB-5 (EE), GFP::RAB-7 (LE) and LMP-1::GFP (Ly). These results indicate that *CalipHluor*$_{A647}$ is present in EE, LE, and Ly at 5 min, 17 min and 60 min, respectively. These time points were used to measure the pH and [Ca^{2+}] in EE, LE and Ly in wild-type worms.

Table S3: Mean pH and free [Ca^{2+}] in EE, LE and Ly of wild type (N2) worms, lysosomes of *catp-6*, *cup-5* +/- and *catp-6* RNAi in *cup-5* +/- worms using *CalipHluor*$_{Ly}$.

Worm	pH	Free [Ca^{2+}] (μM)
EE of N2	6.46 ± 0.07	0.3 ± 0.1
LE of N2	5.95 ± 0.02	0.3 ± 0.1
Ly of N2	5.30 ± 0.02	11 ± 0.8
Ly of *catp-6*	5.47 ± 0.03	1.6 ± 0.4
Ly of *cup-5* +/-	5.15 ± 0.01	40 ± 1.5
Ly of CATP-6 RNAi in *cup-5* +/-	5.50 ± 0.10	16 ± 4.9

Early endosome (EE), Late endosome (LE) and Lysosomes (Ly)

For all experiments n = 15 cells, 50 endosomes; data represent the mean ± s.e.m. Experiments were repeated thrice independently with similar results.

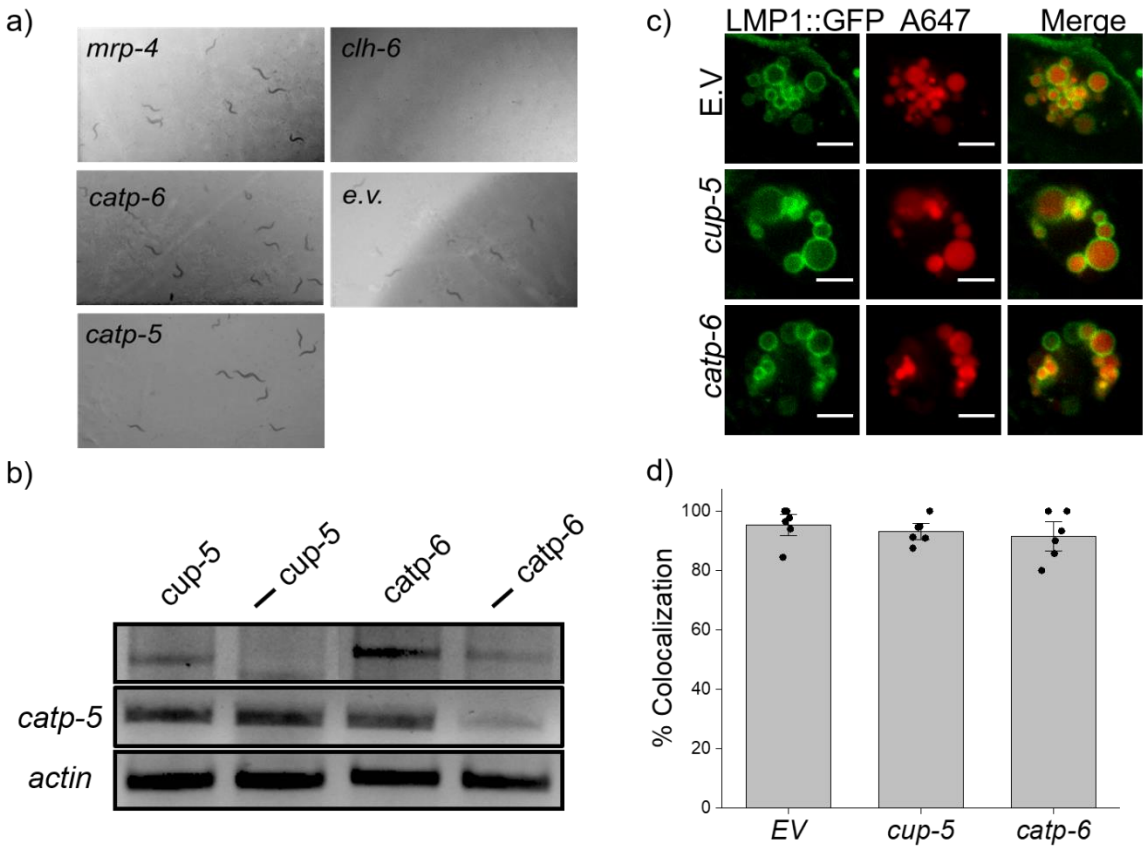

Figure S6. a) *catp-6* rescues the lethality of *cup-5 +/-*. Representative images showing the number of progeny of *cup-5 +/-* worms in plates containing RNAi bacteria of *mrp-4* (positive control), *clh-6*, *catp-6*, *catp-5* and *e.v.* (control). Experiments were repeated twice independently with similar results. b) RT-PCR analysis of total RNA isolated from *C. elegans* pre- and post-RNAi. Lanes correspond to PCR-amplified cDNA of the indicated gene product isolated from wild type without RNAi treatment (denoted by gene name) and the corresponding dsRNA-fed worms (denoted as. '— gene name) c) Representative images of worms expressing LMP-1::GFP (green) in the background of various indicated RNAi, which were injected with *CalipHluor*$_{LyA647}$ (red) and imaged 60 mins post-injection. Scale bar: 5 μm. d) Quantification of colocalization between the *CalipHluor*$_{LyA647}$ and GFP in LMP-1::GFP worms. n=10 cells; error bars represent mean ± s.e.m.

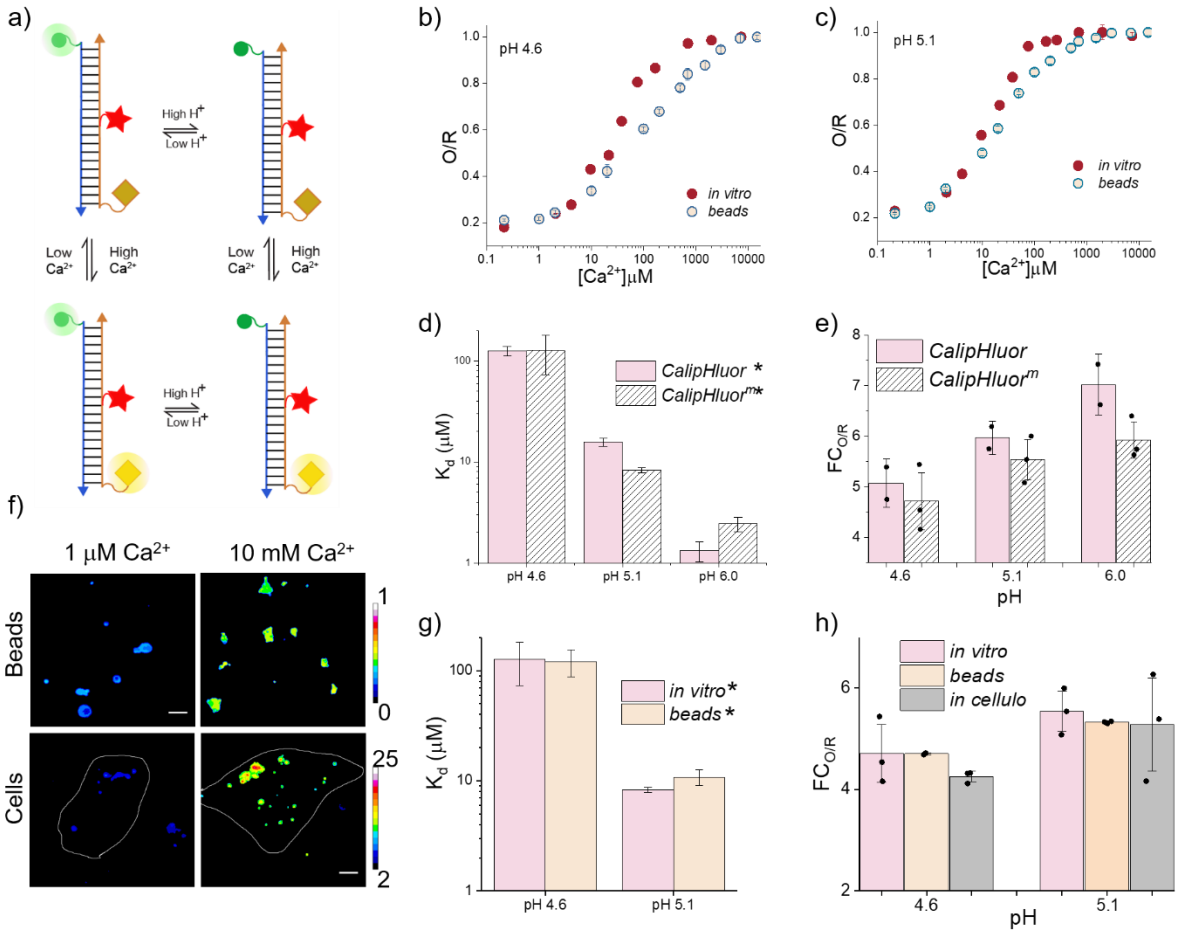

Figure S7: a) Schematic of working principle of *CalipHluor*^{mLy}. An Oregon Green based pH sensor (green sphere) and ion insensitive Alexa647 (acceptor, red star) and a Ca^{2+} sensitive fluorophore (Rhod-5F, yellow diamond). Calibration curves comparing *in vitro* (red) and on beads (orange) calibration at; b) pH 4.6 and c) pH 5.1. Comparison of d) K_d and e) Fold change (FC) in O/R of *CalipHluor*^{Ly} (pink) and *CalipHluor*^{mLy} (black). f) Representative images Comparison of g) Fold change (FC) in O/R and h) K_d of *CalipHluor*^{mLy} *in vitro* (pink), on beads (orange) and *in cellulo* (grey). (n = 5 cells; 30 endosomes; n=60 beads). Experiments were performed thrice independently. * Error is obtained from Hill equation fit. Error bars represent mean $\pm$ s.e.m. Scale bar: 10µm

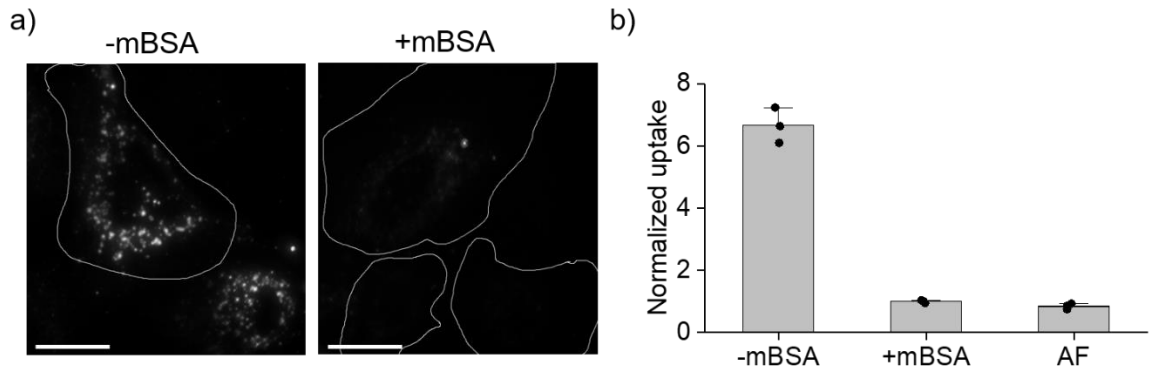

Figure S8: a)-b) *CalipHluor*^{mLy} internalization by primary human skin fibroblasts is competed out by excess maleylated BSA (mBSA, 10 μM), revealing uptake is by scavenger receptors. Cells are imaged in Alexa647 channel. AF: autofluorescence. Scale bar: 10μm. Experiments were performed in triplicate. Error bars indicate the mean of three independent experiments ± s.e.m. (n = 25 cells).

Reference

1. Grynkiewicz, G., Poenie, M. & Tsien, R. Y. A new generation of Ca2+ indicators with greatly improved fluorescence properties. *J. Biol. Chem.* **260,** 3440–3450 (1985).
2. Collot, M. *et al.* CaRuby-Nano: a novel high affinity calcium probe for dual color imaging. *Elife* **4,** (2015).
3. Modi, S. *et al.* A DNA nanomachine that maps spatial and temporal pH changes inside living cells. *Nat. Nanotechnol.* **4,** 325–330 (2009).
4. Moore, D. & Dowhan, D. Purification and concentration of DNA from aqueous solutions. *Curr. Protoc. Mol. Biol.* **Chapter 2,** Unit 2.1A (2002).
5. Brenner, S. The genetics of Caenorhabditis elegans. *Genetics* **77,** 71–94 (1974).
6. Kamath, R. S. & Ahringer, J. Genome-wide RNAi screening in Caenorhabditis elegans. *Methods* **30,** 313–321 (2003).
7. Surana, S., Bhat, J. M., Koushika, S. P. & Krishnan, Y. An autonomous DNA nanomachine maps spatiotemporal pH changes in a multicellular living organism. *Nat. Commun.* **2,** 340 (2011).
8. Evangelidis, G. D. & Psarakis, E. Z. Parametric image alignment using enhanced correlation coefficient maximization. *IEEE Trans. Pattern Anal. Mach. Intell.* **30,** 1858–1865 (2008).
9. Sauvola, J. & Pietikäinen, M. Adaptive document image binarization. *Pattern Recognit* **33,** 225–236 (2000).
10. Schindelin, J. *et al.* Fiji: an open-source platform for biological-image analysis. *Nat. Methods* **9,** 676–682 (2012).
11. C. elegans Deletion Mutant Consortium. large-scale screening for targeted knockouts in the Caenorhabditis elegans genome. *G3 (Bethesda)* **2,** 1415–1425 (2012).
12. Fares, H. & Greenwald, I. Regulation of endocytosis by CUP-5, the Caenorhabditis elegans mucolipin-1 homolog. *Nat. Genet.* **28,** 64–68 (2001).

13. Engelstein, M. *et al.* An efficient, automatable template preparation for high throughput sequencing. *Microb. Comp. Genomics* **3,** 237–241 (1998).
14. Vandeventer, P. E. *et al.* Multiphasic DNA adsorption to silica surfaces under varying buffer, pH, and ionic strength conditions. *J. Phys. Chem. B* **116,** 5661–5670 (2012).